COLLEGE OF ENGINEERING

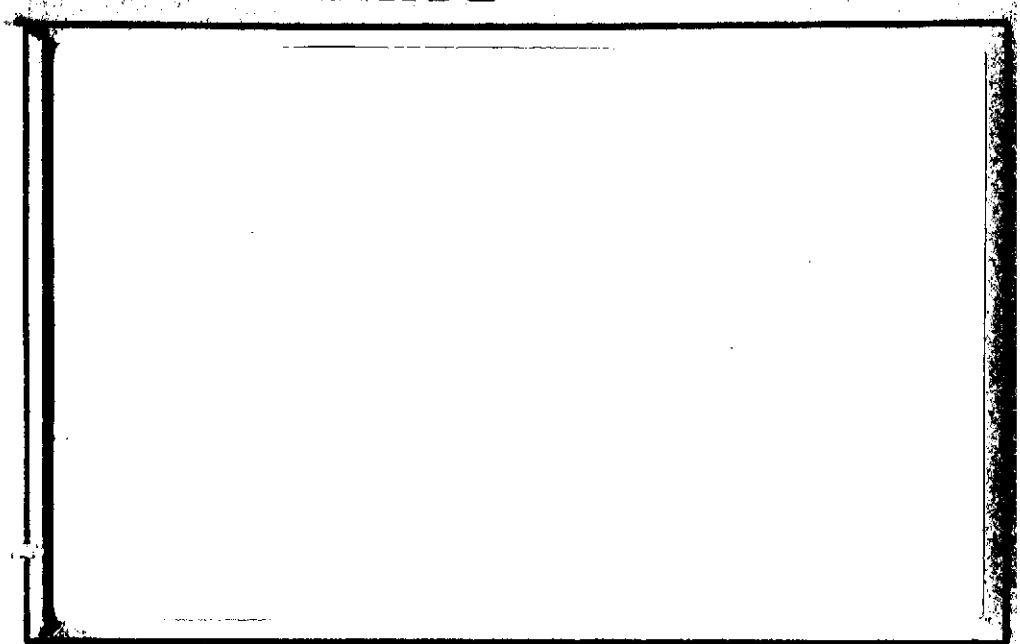

VIRGINIA POLYTECHNIC INSTITUTE AND STATE UNIVERSITY

BLACKSBURG, VIRGINIA

College of Engineering
Virginia Polytechnic Institute & State University
Blacksburg, Virginia 24061

VPI-E-74-1

STRESS INTENSITY FACTORS FOR DEEP CRACKS EMANATING FROM THE CORNER FORMED BY A HOLE INTERSECTING A PLATE SURFACE

J. J. McGowan* and C. W. Smith**

Department of Engineering Science & Mechanics

January 1974

Reporting Period: Fall 1972 through Fall 1973

Prepared For:

National Aeronautics and Space Administration
Grant No. NGR 47-004-476 with
NASA-Langley Research Center, Hampton, Virginia

*Lecturer
**Professor
Department of Engineering Science & Mechanics
Virginia Polytechnic Institute & State University
Blacksburg, Virginia 24061

1. Report No.
VPI-E-74-1

4. Title
STRESS INTENSITY FACTORS FOR DEEP CRACKS EMANATING FROM THE CORNER FORMED BY A HOLE INTERSECTING A PLATE SURFACE

5. Report Date
January 1974

7. Authors
J. J. McGowan and C. W. Smith

8. Performing Organization Report Number
VPI-E-74-1

9. Performing Organization Name & Address
Department of Engineering Science & Mechanics
Virginia Polytechnic Institute & State University
Blacksburg, Virginia 24061

10. Work Unit No.
NASA 1463

11. Contract or Grant No.
NGB 47-004-476

12. Sponsoring Agency Name and Address
NASA
Langley Research Center
Hampton, Virginia

13. Type of Report & Period Covered
Fall '72 -- Fall '73

16. Abstract

A technique consisting of a marriage between stress freezing photo-elasticity and a numerical method was used to obtain stress intensity factors for natural cracks emanating from the corner at which a hole intersects a plate surface. Geometries studied were: crack depth to thickness ratios of approximately 0.2, 0.5 and 0.75; crack depth to crack length ratios of approximately 1.0 to 2.0; and crack length to hole radius ratios of about 0.5 to 2.0. All final crack geometries were grown under monotonic loading and growth was not self similar, with most of the growth occuring through the thickness under remote extension. Stress intensity factors were determined at the intersection of the flaw border (i) with the plate surface (K_S) and (ii) with the edge of the hole (K_H). Results showed that for the relatively shallow flaws $K_H \simeq 1.5K_S$, for the moderately deep flaws $K_H \simeq K_S$ and for the deep flaws $K_H \simeq 0.5K_S$, revealing a severe sensitivity of K to flaw geometry. Results were compared with the Bowie Theory, and approximate criteria developed by Hall and Finger and Hsu and Liu. These comparisons showed that these theories significantly over-estimated the SIF for moderately deep flaws $a/t \simeq 0.5$ at both the plate surface and the hole, but for shallow flaws, and Hall-Finger theory under-estimated the SIF at the hole and the Bowie theory under-estimated the SIF at the surface for deep flaws.

17. Key Words
Stress Intensity Factor, Hole Cracks, Photoelasticity, Fracture Mechanics, Stress Freezing

18. Distribution Statement
Approved for public release; distribution unlimited

19. Security Classif. (report)
Unclassified

20. Security Classif. (page)
Unclassified

NOMENCLATURE

σ_{nn}, σ_{zz}, τ_{nz}	- Stress components in plane normal to crack border (psi)
σ_o	- Normal stress in direction of crack extension near crack tip (psi)
$\bar{\sigma}$	- Remote stress (psi)
K_I	- Mode I stress intensity factor (psi - $[in]^{1/2}$)
r,θ	- Polar coordinates (in, radians)
a	- Flaw depth (in)
c	- Flaw length (in)
r	- Hole radius (in)
t	- Plate thickness (in)
N	- Fringe order
f	- Material fringe value (lbs/in/order) (f_{AVG} = 1.46)
K_S	- Mode I SIF at plate surface (psi - $[in]^{1/2}$)
K_H	- Mode I SIF at hole surface (psi - $[in]^{1/2}$)
K_{Ex}	- Mode I SIF Experimental (psi - $[in]^{1/2}$)
K_{Ap}	- Mode I SIF Apparent (psi - $[in]^{1/2}$)

TABLE OF CONTENTS

INTRODUCTION

A common cracked body problem in the aerospace industry consists of a corner crack emanating from the intersection edge between a plate surface and a hole. No analytical solution exists for this problem even as a near field solution only. Yet the designer is forced to design against this type of crack using very approximate methods [1]. Apparently, the first study undertaken of the problem was an experimental study by Hall and Finger [2]. They inserted artificial flaws by EDM with depth/length less than unity and used fatigue loads to initiate cracks after which residual static strength tests were run. In evaluating their results, they assumed that a state of plane strain existed at the point of intersection of the flaw border and the boundary, but in their fracture criterion they had only one value for the stress intensity factor (SIF) and did not account for the variation of the SIF and constraint along the flaw border. As an alternate approach, they suggested modelling the corner flaw with an "equivalent" Bowie type [3] through crack. The latter approach was refined by Liu [4] but still required the selection of an arbitrary equivalent crack length for the Bowie model. This approach has recently been expanded by Hsu and Liu [5], and while this latter analysis contains some two dimensional approximations, and takes no account of back surface effects, it constitutes the most recent effort at quantifying the problem.

Because of the technological importance of the above problem, and the approximate nature of existing analytical approaches necessitated by the intractability of the mathematical model of the complete problem, one is led to consider experimental techniques as an alternate approach. Stress

freezing photoelasticity is a well known technique for evaluating three dimensional stress distributions in the vicinity of stress raisers. A method for extracting the stress intensity factor from photoelastic data for two dimensional problems was proposed by Irwin [6] in 1953, and the method has been modified and refined substantially since that time. Recent studies by Kobayashi and his associates [7]-[10] have applied the method to dynamic photoelasticity, and the senior author and his associates [11]-[21] have refined the method for three dimensional problems.

It was the purpose of the present study to determine stress intensity factors at the end points of flaws emanating from the corner formed by the intersection of a plate with a hole using stress freezing photoelasticity and to compare the results with the studies noted above. The authors used a numerical technique known as the Taylor Series Correction Method (TSCM) [20] in order to extract the SIF values from the photoelastic data. Before describing the experiments, a brief review of the analytical background appears to be desirable.

ANALYTICAL CONSIDERATIONS

Consider the Irwin two parameter near field equations for Mode I loading:

$$\sigma_{nn} = \frac{K_I}{(2\pi r)^{1/2}} \cos\frac{\theta}{2}\left(1 - \sin\frac{\theta}{2}\sin\frac{3\theta}{2}\right) - \sigma_o$$

$$\sigma_{zz} = \frac{K_I}{(2\pi r)^{1/2}} \cos\frac{\theta}{2}\left(1 + \sin\frac{\theta}{2}\sin\frac{3\theta}{2}\right) \qquad (1)$$

$$\tau_{nz} = \frac{K_I}{(2\pi r)^{1/2}} \sin\frac{\theta}{2}\cos\frac{\theta}{2}\cos\frac{3\theta}{2}$$

where the notation, adapted to the problem at hand, is pictured in Figure 1. Here σ_o is the part of the regular stress field which is independent of r. Although Equations (1) were originally proposed for two dimensional problems, the singular parts have been shown to be valid for stresses in planes perpendicular to elliptically shaped crack borders [22] and are generally applied to arbitrary shaped plane crack borders as well. By substituting Equations (1) into Equation (2):

$$\tau_{max} = \frac{1}{2}[(\sigma_{nn} - \sigma_{zz})^2 + 4\tau_{nz}^2]^{1/2} \tag{2}$$

and evaluating τ_{max} along $\theta = \pi/2$, one obtains:

$$\tau_{max} = [\frac{K_I^2}{8\pi r} + \frac{K_I\sigma_o}{4(\pi r)}1/2 + \frac{\sigma_o^2}{4}]^{1/2} \tag{3}$$

which may be combined with the stress optic law:

$$\tau_{max} = \frac{Nf}{2t} \tag{4}$$

in order to obtain an expression of the form:

$$K_I = f(\sigma_o, N_i, r_i) \tag{5}$$

from which K_I may be evaluated from experimental data N_i, r_i along $\theta = \pi/2$ (See references [16] and [17]) The stresses are evaluated along $\theta = \pi/2$ since the fringes spread out in approximately this direction and can be most accurately discriminated along this line. An alternate form of Equation (3) may be written as:

$$\tau_{max} = \frac{A'}{r^{1/2}} + B_o' + B_1' r^{1/2} \tag{6}$$

where

$$A' = \frac{K_I}{\sqrt{8\pi}} \quad \text{and} \quad B_1' = B_1' (A', B_0')$$

When one accumulates photoelastic data along $\theta = \pi/2$, if the foregoing theory is to hold, the stresses in the data zone must be dominated by the singular stresses as given in Equations (1). Experience with three dimensional problems has revealed that the singular zone is often severely constricted and a part of the data may lie outside that zone. In order to adequately account for this effect, the authors have used a Taylor Series Expansion of the regular part of the maximum in plane shearing stress in the form:

$$\tau_{max} = \frac{A}{r^{T/2}} + \sum_{n=0}^{m} B_n r^{n/2} \qquad (7)$$

where $A = K_I/\sqrt{8\pi}$ as before.

If we ignore the dependence between the coefficients A', B_0', B_1' in Equation (6) we see that Equation (7) reduces to Equation (6) for a two degree of freedom system of equations to within truncation error. Moreover, Equation (7) corresponds to an application of the Williams Stress Function along $\theta = \pi/2$ for two dimensional problems.

In order to apply Equation (7), one determines the coefficients A, B_n from a least squares analysis of the experimental data using a truncated form of Equation (7). Normally the lowest order curve which best fits the experimental data is used. Details are described in references [17] and [21].

THE EXPERIMENTS

Models

A series of stress freezing photoelastic experiments were designed for the purpose of obtaining estimates of the SIF at points S and H along the flaw border. (Figure 1) The specimens were made from PLM-4B, a stress freezing material manufactured by Photolastic, Inc., Malvern, Pa. and Hysol 4290 made by Hysol Corp., Olean, N. Y. using the following procedure:

i) Mill 30 mils from both surfaces of the plates.

ii) Drill and ream holes.

iii) Mount a razor blade in a special jig and tap in a quarter circular crack.

iv) Mount test specimen in a stress freezing oven in a dead loading rig (Figure 2) and heat to critical temperature.

v) Load with enough load to slowly extend flaw to its desired depth. Remove the load.

Test geometries studied are found in the upper part of Table I. It was originally intended to attempt to duplicate the geometries of the Hall and Finger tests. However, since natural cracks were used, only one crack dimension could be controlled, and the other dimension grew to its "natural" companion value. This led to flaws for which $a/c > 1.0$ and self similar flaw extension did not occur. Instead, most of the growth occurred in the depth direction. In one test, (Test 9) a crack with $a/c < 1.0$ was produced by flexing the plate to enlarge the c dimension.

Test Procedure

After crack growth was completed, live loads below the threshold value

to cause crack growth were applied above the critical temperature, and specimens were cooled under load, thus freezing in the fringes and deformations. Slices were then taken i) parallel to the plate surface for use in determining the SIF at point S and ii) tangent to the hole for determining the SIF at point H. The latter slice was sanded on the hole surface to constant thickness. Slice locations are shown in Figure 3. These slices were placed in a tank of liquid of the same index of refraction as the model material and fringe patterns were obtained using partial mirror fringe multiplication and also by the Tardy method. A typical fringe pattern for the hole H is shown in Figure 4. Slices were 0.02 to 0.07 in. thick.

Results

A typical set of data for points S and H are shown in Figure 5 together with the TSCM curves generated from the data. These curves may be regarded as typical of all of the tests analyzed. That is, for all tests, the surface slices revealed linear data which indicates a two degree of freedom system of equations while the slices along the hole revealed non-linear data. For these cases, however, the Tardy method revealed that this data was also linear over a portion of the data zone nearer to the crack tip. Thus, instead of using a higher order curve to fit all of the data, the authors elected to use a two degree of freedom system on that portion of the data in the linear range as shown for the H curve in Figure 5. The authors interpret the linear part of the curve to represent the singular zone and believe that extrapolation of the linear curve results in much less error than would be the case for a higher order curve. In order to verify this technique, a test was run where the corner crack was allowed to grow through the thickness of the

plate so as to form a Bowie type crack on one side of the hole. The hole radius was 0.19 inches and the crack length was 1.15 inches. The resulting K_{Ex} was 2% higher than the result predicted by the Bowie analysis. The authors estimate, however, that experimental results generally can vary by 5%. Even after Tardy analysis, the slopes of the curves of normalized K_{Ap} vs. $(\frac{r}{a})^{1/2}$ or $(\frac{r}{c})^{1/2}$ were, in some cases, sufficiently large to cause the authors some concern as to the accuracy of the K_{HEx} values. In general, the authors estimate that the values of K_{SEx} identified as Experimental Values in Table I, are accurate to within 5% but values of K_{HEx} are, on the average, probably not better than about 15%. Thus, the authors feel that the results for K_{HEx} should be interpreted as trends rather than as exact values. In this context, the experimental results tabulated in Table I may be summarized as follows:

$$\text{For} \left\{ \begin{array}{lcl} a/t & \simeq & 0.2 \\ a/c & = & 1.0 \text{ to } 1.5 \\ c/r & \simeq & 0.5 \\ 2r/t & = & 0.5 \text{ to } 0.9 \end{array} \right\} \quad K_{HEx} \simeq 1.5\, K_{SEx}$$

$$\text{For} \left\{ \begin{array}{lcl} a/t & \simeq & 0.5 \\ a/c & = & 1.0 \text{ to } 1.5 \\ c/r & = & 0.5 \text{ to } 2.0 \\ 2r/t & = & 0.5 \text{ to } 0.9 \end{array} \right\} \quad K_{HEx} \simeq K_{SEx}$$

$$\text{For} \left\{ \begin{array}{lcl} a/t & \simeq & 0.75 \\ a/c & \simeq & 2.0 \\ c/r & = & 0.8 \text{ to } 1.6 \\ 2r/t & = & 0.5 \text{ to } 0.9 \end{array} \right\} \quad K_{HEx} \simeq 0.5\, K_{SEx}$$

Moreover, except for the shallow flaws, for $a/c > 1$, $K_{SEx} > K_{HEx}$. These results show that K_{HEx} drops off and K_{SEx} increases as the cracks grow deeper. This growth trend is believed to be due to a variation in constraint distribution with flaw depth. For the parametric ranges included in this study. a/t seems to be the

the dominant parameter but a/c is also seen to be important, especially for the larger values (i.e., $a/c \to 2.0$). For this reason, the tests are grouped according to a/t values, and within each group are ordered according to increasing values of a/c.

ANALYTICAL COMPARISONS

In the middle of Table I, values of the SIF are estimated for each case tested using the theories of Hall and Finger, Bowie, and Hsu and Liu. (See Appendix A) These results are summarized in abbreviated normalized form in the Sub-Table at the bottom of Table I for purposes of comparison.

In Group II ($a/t \simeq 0.5$, $a/c \simeq 0.9$ to 1.5) all of the theories substantially overestimate the SIF both at the surface and at the hole. Although the overestimates range from 10% to 220%, they seem to average about 30% above the experimental result. These same trends are observed in Group I ($a/t \simeq 0.2$, $a/c \simeq 1$ to 1.5) at the surface and in Group III ($a/t \simeq 0.75$, $a/c \simeq 2.0$) at the hole. However, for Group I at the hole, the Hall-Finger solution underestimates the SIF by about 20%, and for Group III at the surface, the Bowie solution under-estimates the SIF.

As noted earlier, there are many reasons why agreement should not be expected between the several theories and experiments. The Bowie solution is two dimensional and applies to a very different geometry than the cases studied here which are found to be highly geometry dependent. The Hall- Finger approach assumes that fracture initiates at the hole boundary under a state of plane strain constraint and obtains empirical functions from experimental data only for cases where $a/c < 1.0$. The

Hsu-Liu Theory provides a highly empirical modification of the Bowie solution for obtaining the SIF both at the surface and at the hole and neglects the back surface of the plate altogether. As noted earlier, the effect of increasing a/t was to decrease K_H and to increase K_S. The decrease of K_H with increase in a/t was also observed by Hall and Finger as an "unexpected result." The authors conjecture that this result may be due to the fact that, when the crack is deep, a substantial part of the load is transferred to the side of the hole opposite the crack due to the greater stiffness of this part of the plate. The remaining ligament between the crack and the back surface of the plate thus carries a reduced load and this effect is in evidence in the results shown here. Values of a/c are low enough in tests 1, 3 and 4 that some correlation might be expected with the Hall-Finger Criterion. However, differences between that criterion and experimental results run as high as ±20%, indicating that substantial three dimensional effects may be averaged out in the Hall-Finger approach.

PROBLEM CHARACTERIZATION AND CONCLUSIONS

It is clear from the results of the Sub-Table under Table I that none of the theories studied here are (in their published form) suitable for dealing with deep flaws where a/c $\simeq>$ 1.0. It is also clear that this problem is highly three dimensional and strongly geometry dependent. In order to assist the designer in converting these results into an interim design philosphy until further studies can be carried out, the following suggestions are made:

In Reference [1], the crack growth occuring in this type of problem through the thickness is estimated from the SIF for a quarter circular flaw emanating from the corner of a quarter infinite plate. It is clear from the value of $K_{HEX}/\bar{\sigma}\ c^{1/2}$ from the tests in Group I that such a solution should be corrected to account for the stress raiser effect

due to the hole and that this correction should be of the order of 2.0 to 2.5. Although difficult to justify on purely analytical grounds, the correction obtained from the Bowie solution as c→0 by Hsu and Liu appears to be somewhat conservative but not unsuitable here. For Groups II and III, failure to correct for the presence of the hole is apparently more than offset by the load transfer mechanism mentioned earlier. A 20% or so decrease in the value of C in the Hall-Finger criterion would yield fairly accurate K_I estimates for K_H.

Once the crack has grown through the plate thickness, it forms a Bowie Crack for which K_I (or K_S) is accurately predicted by the Bowie Theory. In fact, the use of the Bowie Theory to predict K_S before the crack breaks through to the far side of the plate could be used (if K_B is decreased by about 20%) for Groups I and II. For Group III, the Hsu-Liu Correction would again be necessary.

The problem studied here is a complex, three dimensional problem and the present study can only be expected to identify trends and point the way for future research. The trends and conclusions from the present study may be summarized as follows:

1) Extension of a crack emanating from a corner of intersection of a hole with a plate under monotonically increasing load is not self-similar. (In this work, most of the growth was through the thickness*) As the flaw depth increases K_H decreases and K_S increases.

9) Existing theories and design criteria significantly overestimate the SIF at both the hole and the surface except for shallow flaws at the hole and deep flaws at the surface.

3) As an interim design criterion, the Bowie Theory with magnifications of the type proposed by Hsu and Liu for $a/t \simeq 0.75$ or greater is tentatively

*Test results on fatigue crack growth at U. S. Air Force Materials Laboratory show that, in some cases, significant growth may occur in the plate surface.

recommended. For K_H estimates, a Hall-Finger approach with adjusted coefficients and relationships is suggested.

The authors are planning to extend the current study to other crack geometries with and without hole fasteners in the near future.

ACKNOWLEDGEMENTS

The authors wish to acknowledge the studies of L. R. Hall, R. W. Finger, T. M. Hsu, A. F. Liu and O. W. Bowie, upon whose work they have drawn. They are also indebted to J. C. Newman for his suggestions and to the staff and facilities of the Engineering Science and Mechanics Department of Virginia Polytechnic Institute and State University. This research was supported by NASA under NGR-47-004-07C with NASA Langley, Hampton, Virginia.

REFERENCES

1. Wilhem, D. P., "Fracture Mechanics Guidelines for Aircraft Structural Applications", AFFDL-TR-69-111, U.S. Air Force Flight Dynamics Laboratory, Wright-Patterson AFB, Ohio, Feb. 1970.

2. Hall, L. R. and Finger, R. W., "Fracture and Fatigue Growth of Partially Embedded Flaws", Proc. of Air Force Conference on Fatigue and Fracture of Aircraft Structures and Materials, AFFDL-TR-70-144, U.S. Air Force Systems Command, Wright-Patterson AFB, Ohio, 235-262, Sept. 1970.

3. Bowie, O. L., "Analysis of an Infinite Plate Containing Radial Cracks Originating at the Boundary of an Internal Circular Hole", J. of Mathematics and Physics, 35, 60-71, (1956).

4. Liu, A. F., "Stress Intensity Factor for a Corner Flaw", J. of Engineering Fracture Mechanics, 4,1, 175-179, March 1972.

5. Hsu, T. M. and Liu, A. F., "Stress Intensity Factors for Truncated Elliptical Cracks", Seventh National Symposium on Fracture Mechanics, College Park, Md., Aug. 27-29, 1973.

6. Irwin, G. R., Discussion of the paper "The Dynamic Stress Distribution Surrounding a Running Crack -- A Photoelastic Analysis", by A. A. Wells and D. Post, Proceedings Society for Experimental Stress Analysis 16, 1, 69-96 (1958).

7. Bradley, W. B. and Kobayashi, A. S., "An Investigation of Propagating Cracks by Dynamic Photoelasticity," J. of Experimental Mechanics 10, 3, 106-113, (March 1970).

8. Bradley, W. B. and Kobayashi, A. S., "Fracture Dynamics -- A Photoelastic Investigation," J. of Engineering Fracture Mechanics 3, 3, 317-332 (October 1971).

9. Kobayashi, A. S., Wade, B. G., Bradley, W. B., and Chiu, S. T., "Crack Branching in Homalite -- 100 Sheets", TR-13, Dept. of Mechanical Engineering, College of Engineering, University of Washington, Seattle, Wash. (June 1972).

10. Kobayashi, A. S. and Wade, B. G., "Crack Propagation and Arrest in Impacted Plates", TR-14, Dept. of Mechanical Engineering, College of Engineering, University of Washington, Seattle, Wash. (July 1972).

11. Smith, D. G. and Smith, C. W., "A Photoelastic Evaluation of the Influence of Closure and Other Effects upon the Local Bending Stresses in Cracked Plates", International Journal of Fracture Mechanics 6, 3, 305-318 (Sept. 1970).

12. Smith, D. G. and Smith, C. W., "Influence of Precatastrophic Extension and Other Effects on Local Stresses in Cracked Plates Under Bending Fields", Experimental Mechanics 11, 9, 394-401 (Sept. 1971).

13. Smith, D. G. and Smith, C. W., "Photoelastic Determination of Mixed Mode Stress Intensity Factors", VPI-E-70-16, June 1970. J. of Engineering Fracture Mechanics 4, 2, 357-366, (June 1972).

14. Marrs, G. R. and Smith, C. W., "A Study of Local Stresses Near Surface Flaws in Bending Fields", Stress Analysis and Growth of Cracks, ASTM STP 513, 22-36 (Oct. 1972).

15. Schroedl, M. A., McGowan, J. J. and Smith, C. W., "An Assessment of Factors Influencing Data Obtained by the Photoelastic Stress Freezing Technique for Stress Fields Near Crack Tips", J. of Engineering Fracture Mechanics 4, 4, Dec. 1972.

16. Schroedl, M. A. and Smith C. W., "Local Stresses Near Deep Surface Flaws Under Cylindrical Bending Fields", VPI-E-72-9 (In Press) Progress in Flaw Growth and Fracture Toughness Testing, ASTM STP 536, Oct. 1973.

17. Schroedl, M. A., McGowan, J. J. and Smith, C. W., "Determination of Stress Intensity Factors From Photoelastic Data With Application to Surface Flaw Problems, VPI-E-73-1, (Feb 1973), Fall Meeting Society For Experimental Stress Analysis, Oct. 1973.

18. Harms, A. E. and Smith, C. W., "Stress Intensity Factors in Long Deep Surface Flaws in Plates Under Extensional Fields VPI-E-73-6 (Feb 1973), Tenth Anniversary Meeting of Society for Engineering Science, Raleigh, N. C. Nov. 1973.

19. Schroedl, M. A. and Smith, C. W. "Influence of Three Dimensional Effects on the Stress Intensity Factor for Compact Tension Specimens" VPI-E-73-15, 20 pages, April 1973 Seventh National Symposium on Fracture Mechanics, College Park, Md., Aug. 1973.

20. Smith, C. W., "Use of Three Dimensional Photoelasticity in Fracture Mechanics" (Invited Paper) Third International Congress on Experimental Mechanics, Los Angeles, Calif., May 13-18, 1973 (In Press), Conference Proceedings and J. of Experimental Mechanics.

21. Schroedl, M. A., McGowan, J. J. and Smith, C. W., "Use of a Taylor Series Correction Method in Photoelastic Stress Intensity Determinations" VPI-E-73-34

APPENDIX A - Related Theoretical Solutions

Two approximate theories have been proposed for the problem described in the foregoing and the two dimensional theory of Bowie was also used. These theories will be briefly described here and their limitations noted.

I. The Bowie Solution [3] -- Bowie utilized conformal mapping in order to obtain a solution to the two dimensional problem of a through crack emanating from a hole under remote extension. The mapping function was constructed by considering separately the transformation between two upper half planes which carries the real axis of one into the real axis interrupted by branch cuts of finite length of the other, and the transformation which maps each of these half planes into circles and their exteriors. The mapping function used was the product transformation and it was approximated by a polynomial. The resulting SIF for a single crack normal to a field of remote uniaxial tension may be expressed as

$$K_I = \bar{\sigma}\sqrt{\pi L}\, F(\tfrac{L}{r}) \qquad \text{(A-1)}$$

where

$\bar{\sigma}$ is the remote tension normal to the crack

L is the crack length

r is the hole radius

$F(\frac{L}{r})$ is numerically evaluated.

II. Hall and Finger [2] -- These investigators prepared a series of test specimens in accordance with Table A-1. Notches were inserted using an EDM and specimens were fatigued to start the cracks. Residual

static strength tests were then conducted. Hall and Finger then postulated that catastrophic fracture would originate at the intersection of the flaw border with the hole and that this region would be under a plane strain type of constraint. On this basis they proposed, as a fracture criterion:

$$\bar{\sigma}\sqrt{a}\, f(a,c,r,t) = K_{Ic} \qquad \text{(A-2)}$$

Then, on the basis of parametric crossplots they refined Equation (A-2) into the form:

$$C\bar{\sigma}\sqrt{a}\, F(\frac{c}{2r}) \cdot G(\frac{a}{t}) \cdot H(\frac{r}{t}) = K_{Ic} \qquad \text{(A-3)}$$

where C=1.1, $H(\frac{r}{t}) = 2\sqrt{r/t}$, and F and G were obtained graphically from the test data. They obtained agreement with test data to within 10%. Two points however, should be noted:

(1) Since C, F, G and H were obtained from the test data, Eq. A-3 is necessarily limited to the range of test data which includes no $a/c > 1.0$.

(2) While the assumption that plane strain constraint exists at the point where the flaw intersects the boundary is certainly the safe, logical assumption to make for a design criterion, and seems to yield reasonable results in their work, the complex variation in K_I and the constraint along the flaw boundary is masked by this assumption so that one would not be surprised to see deviations from this criterion for other geometries. Nevertheless, this study should be useful in establishing trends due to variations in test geometry.

III. Hsu and Liu [5] -- These investigators modified the elliptic flaw solution to the form:

$$K_I = \frac{\bar{\sigma}\sqrt{\pi b} \cdot B \cdot M_1'}{\Phi} \qquad \text{(A-4)}$$

where:

b = c in the notation of this paper.

B = factor which corrects crack solution for the presence of the hole. It consists of F(L/r) in I.

$M_1' = M_1\{(\frac{c}{a})^2 \sin^2\beta + \cos^2\beta\}^{1/4}$ where M_1 is a front surface correction factor and β is measured from the front surface to a point on the flaw border.

$$\Phi = \int_0^{\pi/2} \left\{ 1 - \left(\frac{a^2 - c^2}{a^2}\right) \sin^2\beta \right\}^{1/2} d\beta$$

Unfortunately, no attempt was made to account for the influence of the back surface of the plate upon the stress intensity factors. Moreover, the analytical basis for the B factor is two dimensional and it's variation along the flaw border is quite arbitrary and empirical.

TABLE A-1*

TEST PROGRAM FOR FLAWS ORIGINATING AT HOLES

Test Temp. (°F)	$\frac{2r}{t}$	$\frac{a}{t}$	Number of Tests For a/c =		
			0.25	0.50	1.00
-320 2219-T87 AL.	1.0	0.2	2	2	2
		0.5	2	2	2
		0.8	2	2	2
	0.5	0.2	2	2	2
		0.5	2	2	2
		0.8	2	2	2
-320 Ti. -5Al -2.5Sn	1.0	0.2	2	2	2
		0.5	2	2	2
		0.8	2	2	2
	0.5	0.2	2	2	2
		0.5	2	2	2
		0.8	2	2	2

*From Reference [2]

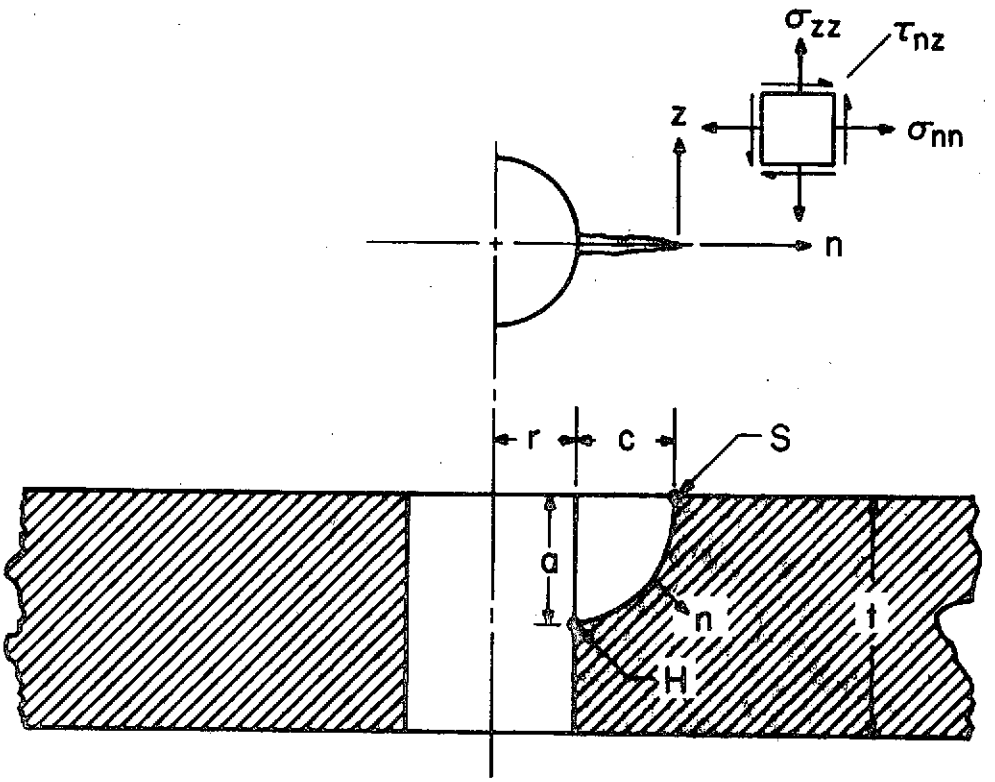

Figure 1 - Problem Geometry and Stress Notation

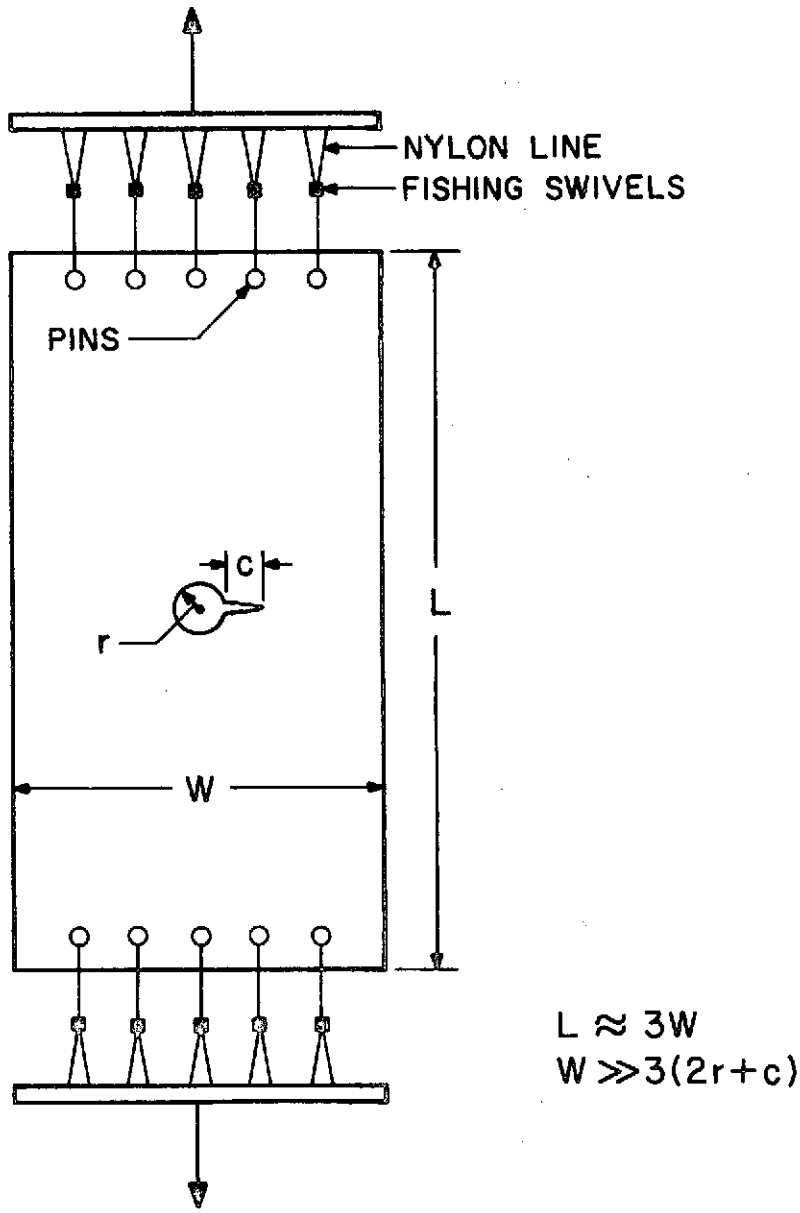

Figure 2 - Test Setup

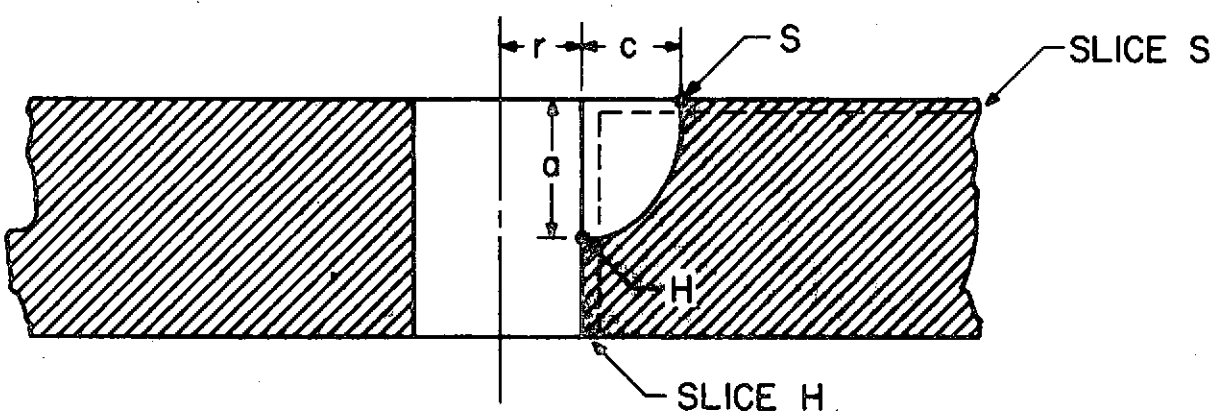

Figure 3 - Slice Locations

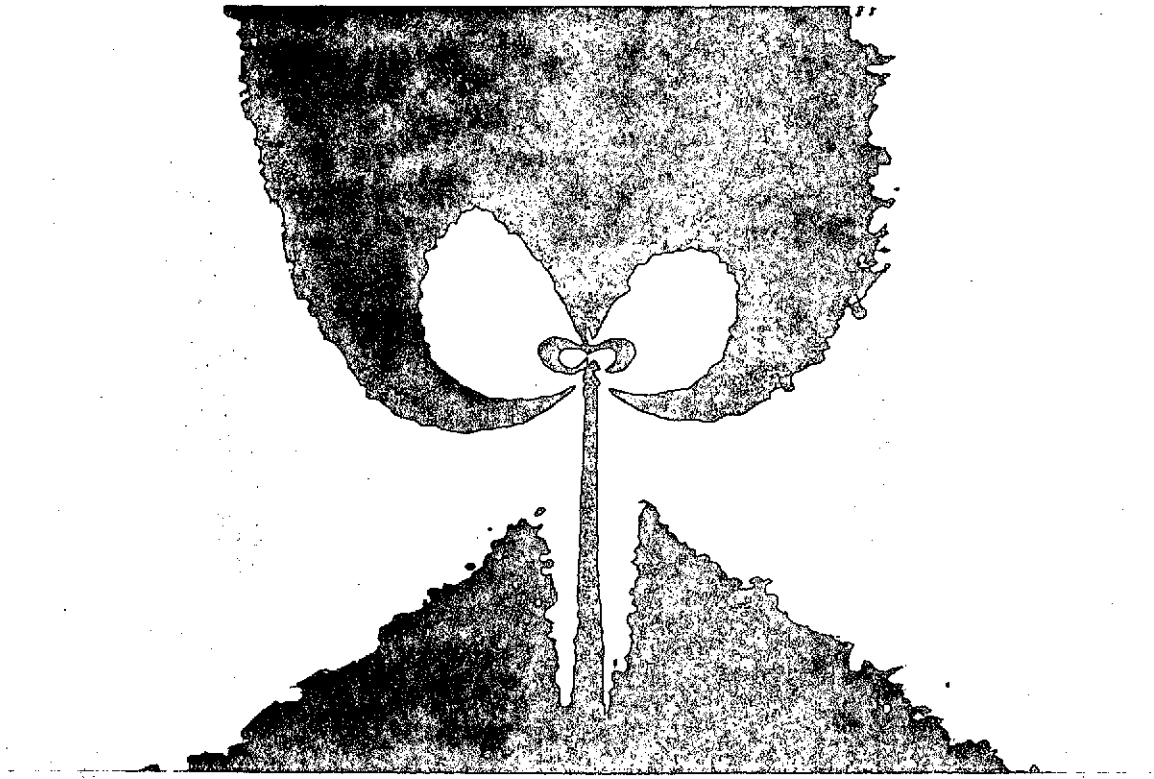

(a) unmultiplied

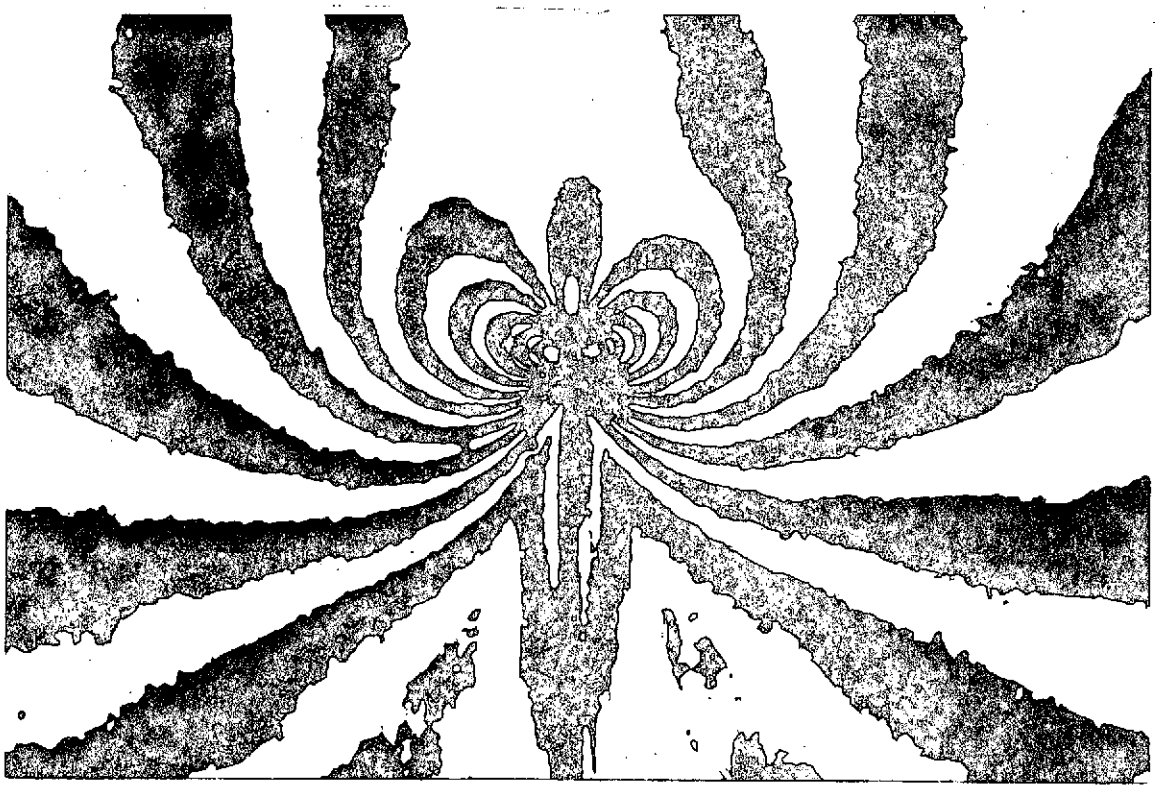

(b) 5th multiple

Figure 4. Typical Fringe Patterns
(Dark Field, 15X)

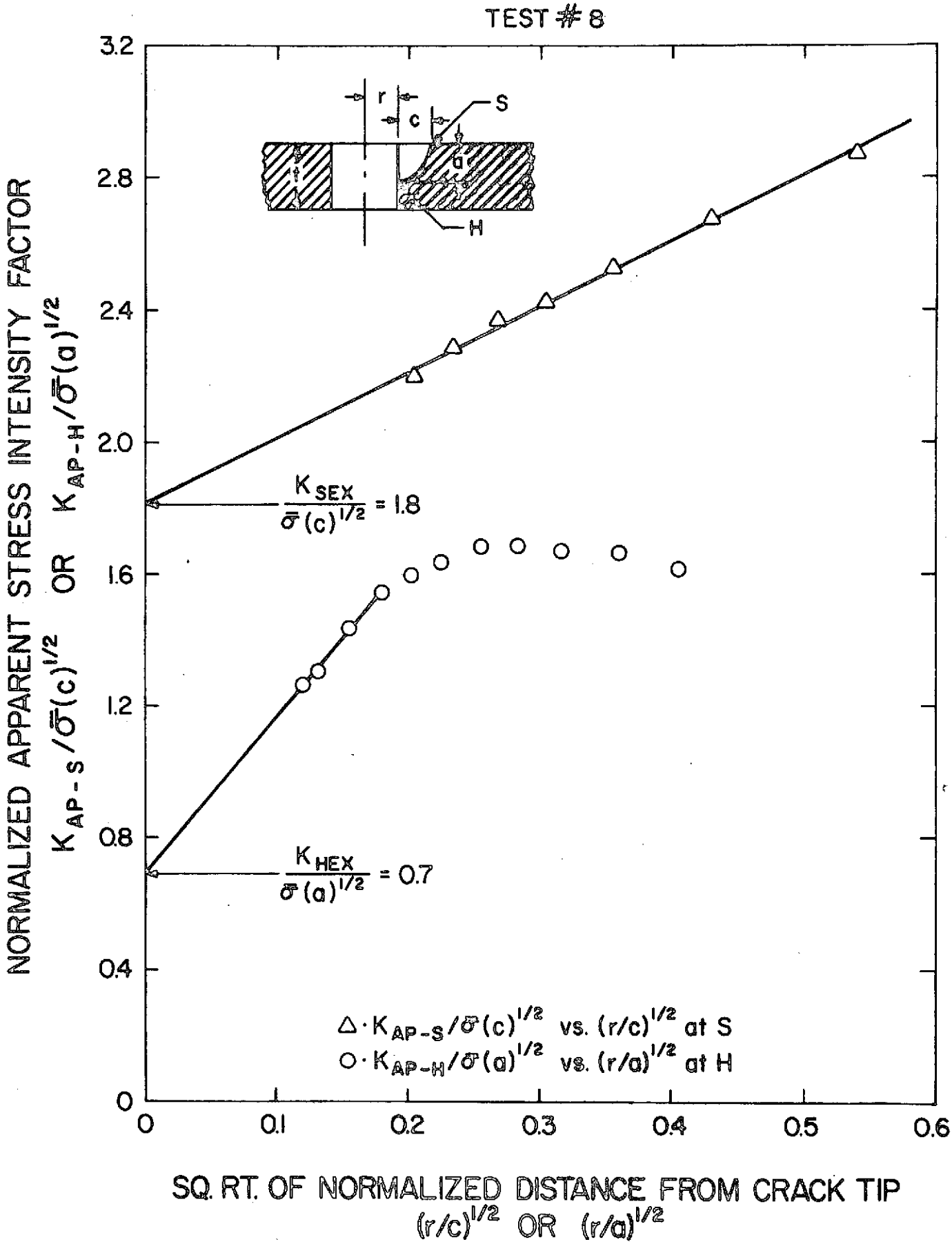

Figure 5 - Typical Data and Results

TABLE I - DATA AND RESULTS

	Group I		Group II				Group III		
Test Number	1	2	3	4	5	6	7	8	9
Hole Radius (r) in.	0.25	0.25	0.19	0.25	0.19	0.25	0.25	0.19	0.19
Plate Depth (t) in.	0.58	0.93	0.76	0.57	0.78	0.54	0.53	0.78	0.78
Crack Length (c) in.	0.11	0.14	0.38	0.25	0.30	0.16	0.20	0.29	1.02
Crack Depth (a) in.	0.10	0.22	0.33	0.27	0.38	0.25	0.39	0.60	0.42
Remote Stress ($\bar{\sigma}$) psi	14.38	15.62	12.34	10.81	11.70	12.78	10.27	8.92	7.06
a/t	0.18	0.24	0.43	0.48	0.49	0.46	0.74	0.78	0.55
a/c	0.95	1.59	0.86	1.10	1.27	1.55	1.98	2.05	0.42
c/r	0.43	0.56	2.02	0.98	1.60	0.63	0.79	1.56	5.44
2r/t	0.87	0.54	0.49	0.88	0.48	0.94	0.95	0.48	0.48
Stress Intensity Factors: Experimental Results									
Surface K_{SEx} psi-in$^{1/2}$	9.43	12.84	8.89	8.97	7.35	10.00	12.23	8.79	6.89
Hole K_{HEx} psi-in$^{1/2}$	13.88	18.26	9.31	8.86	7.15	10.53	7.54	4.77	*
Empirical Results									
Hall-Finger K_{HF} psi-in$^{1/2}$	10.85	13.57	11.30	10.59	10.37	11.92	10.23	8.81	8.23
Bowie K_B psi-in$^{1/2}$	12.13	13.80	11.37	10.44	10.52	11.49	9.56	7.99	8.07
Hsu-Liu (Surf.) K_{HLS} psi-in$^{1/2}$	12.19	16.25	11.53	11.03	11.95	13.41	11.75	9.76	5.56
Hsu-Liu (Hole) K_{HLH} psi-in$^{1/2}$	17.06	20.07	27.80	19.38	22.94	17.64	15.09	16.45	24.00

SUB-TABLE

Test Number	1	2	3	4	5	6	7	8	9
$K_{SEx}/\bar{\sigma}c^{1/2}$	2.0	2.2	1.2	1.7	1.2	2.0	2.7	1.8	1.0
$K_B/\bar{\sigma}c^{1/2}$	2.6	2.4	1.5	2.0	1.6	2.3	2.1	1.7	1.1
$K_{HLS}/\bar{\sigma}c^{1/2}$	2.6	2.8	1.5	2.1	1.9	2.6	2.6	2.0	0.8
$K_{HEx}/\bar{\sigma}a^{1/2}$	3.0	2.5	1.3	1.6	1.0	1.7	1.2	0.7	*
$K_{HF}/\bar{\sigma}a^{1/2}$	2.4	1.9	1.6	1.9	1.4	1.9	1.6	1.2	1.8
$K_{HLH}/\bar{\sigma}a^{1/2}$	3.7	2.7	4.0	3.5	3.2	2.8	2.4	2.4	5.2

*dropped due to data scatter